UDC 629.544:629.5.015

Ivo SENJANOVIĆ[1]
Nikola VLADIMIR[1]
Dae SEUNG CHO[2]

Application of 1D FEM & 3D BEM Hydroelastic Model for Stress Concentration Assessment in Large Container Ships

Original scientific paper

Ultra Large Container Ships (ULCS) have relatively lower torsional stiffness and higher speed, compared to the other merchant ships. Due to their specific design and operational characteristics, natural frequencies of ULCS can fall into the range of encounter frequencies of ocean wave. So, their structural design should be based on hydroelastic analysis. In this paper an outline of an earlier developed hydroelastic model, comprised of a sophisticated beam structural model and a 3D panel hydrodynamic model, is given. The sophisticated beam model includes shear influence on both bending and torsion, contribution of transverse bulkheads to hull stiffness as well as an appropriate modelling procedure of relatively short engine room structure. The model represents a reliable numerical tool for determination of ship global hydroelastic response in frequency domain, by the modal superposition method and here a possibility of its extension for stress concentrations assessment, as a prerogative for fatigue damage calculation, is shown. The procedure is illustrated within the numerical example which includes complete hydroelastic analysis of an 11400 TEU container ship. The transfer functions of sectional forces are determined and compared to the rigid body response. Further on, modal displacements at selected cross-sections are calculated, and then they are spread to the fore and aft contour of a fine 3D FEM substructure model. Finally, the stress concentrations in the considered structural detail are obtained. The validation of the sophisticated beam model is done by correlation analysis with the dry natural vibration response of the fine mesh 3D FEM model. Global and local hydroelastic responses are compared with those calculated by the fully coupled 3D FEM + 3D BEM hydroelastic model and acceptable agreement is obtained.

Keywords: *beam model, container ship, hydroelasticity, springing, stress concentrations, substructure*

Primjena 1D FEM i 3D BEM hidroelastičnog modela u analizi koncentracije naprezanja velikih kontejnerskih brodova

Izvorni znanstveni rad

U usporedbi s drugim trgovačkim brodovima, ultra veliki kontejnerski brodovi imaju relativno manju krutost na uvijanje i veću brzinu. Zbog specifičnih projektnih i eksploatacijskih značajki ultra velikih kontejnerskih brodova, njihove prirodne frekvencije mogu zaći u područje susretnih frekvencija, te stoga osnivanje konstrukcije takvih brodova treba biti utemeljeno na hidroelastičnoj analizi. U članku je ukratko prikazan ranije razvijeni model za hidroelastičnu analizu, koji se sastoji od sofisticiranog grednog strukturnog i 3D panelnog hidrodinamičkog modela. Sofisticirani gredni model uzima u obzir utjecaj smicanja na savijanje i na uvijanje, doprinos poprečnih pregrada krutosti brodskog trupa i odgovarajući postupak modeliranja relativno kratke konstrukcije strojarnice. Hidroelastični model predstavlja pouzdan numerički alat za analizu globalnog odziva broda u frekvencijskom području koristeći metodu superpozicije prirodnih oblika vibriranja, a u članku je prikazana mogućnost njegova proširenja za analizu koncentracije naprezanja u kritičnim detaljima konstrukcije, kao preduvjet za proračun zamornog oštećenja. Primjena postupka ilustrirana je numeričkim primjerom koji uključuje cjelovitu hidroelastičnu analizu kontejnerskog broda nosivosti 11400 kontejnera. Određene su prijenosne funkcije presječnih sila koje su uspoređene s odzivom krutog broda. Nadalje, izračunati su modalni pomaci na odabranim presjecima, a zatim su raspršeni na pramčanu i krmenu konturu 3D FEM modela podstrukture s ufinjenom mrežom. Naposljetku, određena je koncentracija naprezanja u odabranim detaljima konstrukcije. Validacija grednog modela provedena je usporedbom rezultata analize prirodnih vibracija u zraku s rezultatima dobivenim 3D FEM modelom cijelog broda. Globalni i lokalni hidroelastični odzivi uspoređeni su s odzivima dobivenim s potpuno spregnutim 3D FEM + 3D BEM hidroelastičnim modelom, pri čemu je postignuto prihvatljivo podudaranje.

Ključne riječi: *gredni model, hidroelastičnost, koncentracija naprezanja, kontejnerski brod, potkonstrukcija, pruženje*

Authors' addresses (Adrese autora):
[1] *University of Zagreb, Faculty of Mechanical Engineering and Naval Architecture*, Ivana Lučića 5, 10000 Zagreb, Croatia, ivo.senjanovic@fsb.hr, nikola.vladimir@fsb.hr
[2] *Dept. of Naval Architecture and Ocean Engineering, Pusan National University*, 30 Jangjeon-dong, Guemjeong-gu, Busan, Korea, daecho@pusan.ac.kr

Received (Primljeno): 2012-03-16
Accepted (Prihvaćeno): 2012-05-16
Open for discussion (Otvoreno za raspravu): 2013-12-31

1 Introduction

The increase in world trade has largely contributed to the expansion of sea traffic. As a result, the market demand is leading to Ultra Large Container Ships (ULCS), with expected capacity up to 18000 TEU and length of about 400 m, without changes of the operational requirements (speed around 27 knots). The particular structural design of the container ships-leads to open midship sections, resulting in increased sensitivity to torsional and horizontal bending loads, which is much more complex to simulate numerically [1]. At the same time, due to their large dimensions, the structural natural frequencies of ULCS become significantly lower so that the global hydroelastic structural responses (springing & whipping) can become a critical issue in the ship design and should be properly modelled by the simulation tools since the present Classification Rules do not cover described operating stages completely [1]. Hydroelastic theories for marine structures are reviewed in [2,3]. According to [4,5] the methodology of hydroelastic analysis includes the definition of the structural model, ship and cargo mass distributions, and geometrical model of ship surface. First, dry natural vibrations are calculated, and then modal hydrostatic stiffness, added mass, damping, and wave load are determined. Finally, wet natural vibrations as well as the transfer functions (RAO – response amplitude operator) for determining ship structural response to wave excitation are obtained [4,5]. The hydroelastic problem can be solved at different levels of complexity and accuracy. The best, but highly time-consuming way is to consider 3D FEM structural model and 3D hydrodynamic model based on the radiation-diffraction theory. However, in this paper the sophisticated beam model is coupled with 3D hydrodynamic model that is especially appropriate for the preliminary strength assessment. The paper deals with the application of an existing hydroelastic model for determination of stress concentration transfer functions which are necessary for assessment of fatigue damage/life of ship structural details. Detailed description of the procedure is given in [6], where determining stress concentration transfer function represents a first step in the fatigue damage assessment procedure. After the global hydroelastic response is calculated in the frequency domain using beam structural model, the modal displacements are imposed to the 3D FEM fine mesh substructure model and stress concentration RAOs in the considered structural detail is obtained. The global and local hydroelastic responses are finally verified through the comparison with those obtained by fully coupled 3D FEM + 3D BEM hydroelastic model.

2 Mathematical model

2.1 Structural model outline

As mentioned above, a structural model for hydroelastic analysis can be either a beam model based on the advanced theory of thin-walled girders, which is described in details in [7], or a 3D FEM model as shown in Figure 1.

The beam model can give quite accurate results because it takes shear influence on bending, shear influence on torsion, contribution of transverse bulkheads as well as contribution of relatively short engine room structure to the ship hull global stiffness, in a reliable way.

Total beam deflection and twist angle consist of pure bending and torsion respectively, and shear contribution [7]

$$w = w_b + w_s = w_b - \frac{EI_b}{GA_s}\frac{\mathrm{d}^2 w_b}{\mathrm{d}x^2}, \tag{1}$$

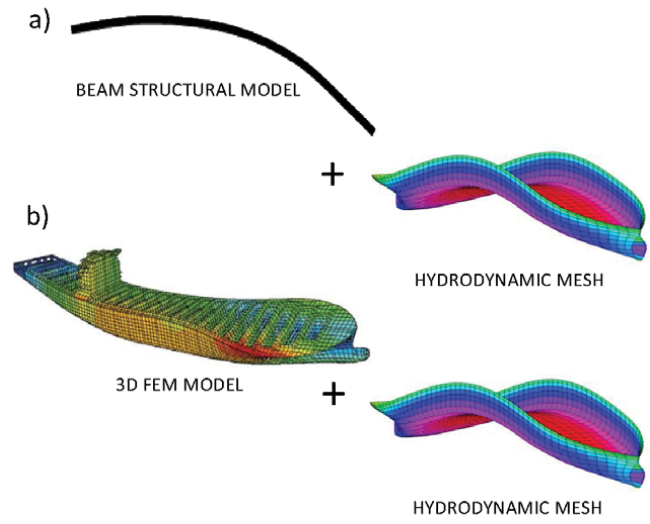

Figure 1 **Schematic presentation of different hydroelastic models; a) beam hydroelastic model, b) fully coupled 3D hydroelastic model**
Slika 1 **Shematski prikaz različitih modela za hidroelastičnu analizu; a) gredni hidreolastični model, b) potpuno spregnuti 3D hidroelastični model**

$$\psi = \psi_t + \psi_s = \psi_t - \frac{EI_w}{GI_s}\frac{\mathrm{d}^2\psi_t}{\mathrm{d}x^2}, \tag{2}$$

where I_b is moment of inertia of cross-section, A_s is shear area, I_w is warping modulus and I_s is shear inertia modulus. E and G are Young's and shear modulus respectively. One can see that there is an analogy between bending and torsion [7,8,9,10]

$$A_s = \frac{Q^2}{\int_A \tau_Q^2 \mathrm{d}A}, \tag{3}$$

$$I_s = \frac{T_w^2}{\int_A \tau_w^2 \mathrm{d}A}, \tag{4}$$

where Q and T_w are shear force and torque due to restrained warping, and τ_Q and τ_w are corresponding shear stresses.

The effect of the large number of transverse watertight and support bulkheads can be incorporated into the hull torsional stiffness [11]

$$I_t^* = \left[1 + \frac{a}{l_1} + \frac{4(1+\nu)C}{I_t l_0}\right] I_t, \quad C = \frac{U}{E\psi_t'^2}, \tag{5}$$

where, according to Figure 2, a is the web height of bulkhead girders, l_0 is the bulkhead spacing, $l_1 = l_0 - a$ is the net length, C is the energy coefficient, ν represents Poisson's ratio, and U is the bulkhead grillage and stool strain energy due to warping of cross-section. Warping shape function can be assumed with the following expression:

$$\bar{u}(y,z) = -y\left\{(z-d) + \left[1-\left(\frac{y}{b}\right)^2\right]\frac{z^2}{H}\left(2-\frac{z}{H}\right)\right\}, \quad (6)$$

$$u(y,z) = \bar{u}(y,z)\psi_t', \quad (7)$$

where H is the ship height, b is one half of bulkhead breadth, d is the distance of warping centre from double bottom centroid, while y and z are transverse and vertical coordinates respectively.

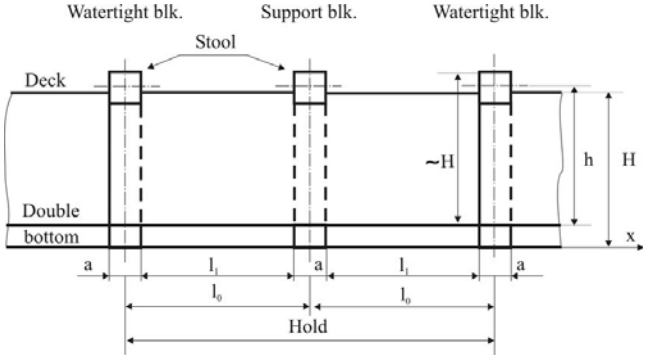

Figure 2 **Longitudinal section of container ship hold [11]**
Slika 2 **Uzdužni presjek kroz skladište kontejnerskog broda [11]**

The bulkhead grillage strain energy includes vertical and horizontal bending with contraction, and torsion [11]

$$U_g = \frac{1}{1-\nu^2}\left[\frac{116H^3}{35b}i_y + \frac{32b^3}{105H}i_z + \frac{8Hb}{75}\nu\left(i_y+i_z\right) + \frac{143Hb}{75}\left(1-\nu\right)i_t\right]E\psi'^2 \quad (8)$$

where i_y, i_z and i_t are the average moments of inertia of cross-section and torsional modulus per unit breadth respectively. The stool strain energy is comprised of the bending, shear and torsional contributions

$$U_s = \left[\frac{12h^2 I_{sb}}{b} + 72\left(1+\nu\right)\frac{h^2}{b^3}\frac{I_{sb}^2}{A_s} + \frac{9bI_{st}}{10\left(1+\nu\right)}\right]E\psi'^2, \quad (9)$$

where I_{sb}, A_s and I_{st} are the moment of inertia of cross-section, shear area, and torsional modulus, respectively. Quantity h is the stool distance from the inner bottom.

Ultra Large Container Ships are also characterized by the relatively short engine room structure with the length of about a half of the ship breadth. Due to its shortness, such kind of engine room structure does not behave like a segment of closed cross-section, but behaves like the open one with increased torsional stiffness due to decks contribution. Details of the mathematical model for engine room structure effective stiffness are presented in [12], and here only the basic expressions are outlined. The effective torsional modulus which includes both open cross-section and deck segments can be written in the form:

$$\tilde{I}_t = \left(1+C\right)I_t^\circ, \quad (10)$$

where I_t° is the torsional stiffness of an open cross-section segment and C is energy coefficient, similarly as in the case of transverse bulkheads, which is calculated according to the following formula:

$$C = \frac{\sum E_i}{E_t} = \frac{4\left(1+\nu\right)t_1\left(\frac{a}{b}\right)^3\left(\left|w_D\right|+\left|w_B\right|\right)^2 k}{\left[1+2\left(1+\nu\right)\left(\frac{a}{b}\right)^2\right]I_t^\circ a}, \quad k = \sum\frac{V_i}{V_1}\left(\frac{h_i}{h_1}\right)^2, \quad (11)$$

where V_i represents the volume of particular deck, w_D and w_B are the values of deck and bottom warping functions respectively. Other geometric quantities in the above formula are illustrated in Figure 3.

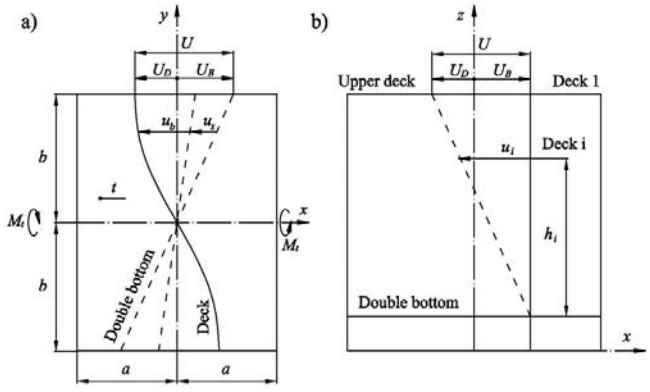

Figure 3 **Engine room deck deformation and double bottom rotation, a) bird's eye view, b) lateral view [12]**
Slika 3 **Deformacija gornje palube i zakretanje dvodna strojarnice; a) pogled odozgo, b) bočni pogled [12]**

The well-known governing matrix equation of dry natural vibrations in a FEM analysis yields

$$\left(\mathbf{K} - \Omega^2\mathbf{M}\right)\boldsymbol{\delta} = \mathbf{0}, \quad (12)$$

where $\mathbf{K}$ is stiffness matrix, $\mathbf{M}$ is mass matrix, Ω is dry natural frequency and $\boldsymbol{\delta}$ is dry natural mode. As solution of the eigenvalue problem (12), Ω_i and $\boldsymbol{\delta}_i$ are obtained for each the i-th dry mode, where $i = 1,2,...,N$, N is total number of degrees of freedom. The first six natural frequencies Ω_i corresponding to the rigid body modes are zero. If 1D analysis is applied, as in the case of the hydroelastic model used in this investigation, the beam vibration modes should be spread to the ship wetted surface. The general expression for spreading nodal displacements to the wetted surface (valid for vertical and coupled horizontal and torsional vibrations) yields:

$$\mathbf{h} = \left[\frac{\mathrm{d}w_v}{\mathrm{d}x}\left(Z-z_N\right) + \frac{\mathrm{d}w_h}{\mathrm{d}x}Y + \bar{u}\frac{\mathrm{d}\psi}{\mathrm{d}x}\right]\mathbf{i} + \left[-w_h - \psi\left(Z-z_S\right)\right]\mathbf{j} + \left[-w_v + \psi Y\right]\mathbf{k}. \quad (13)$$

where w_v is hull vertical deflection, w_h is hull horizontal deflection, ψ is twist angle, Y and Z are global coordinates of the point

on ship surface, and z_N and z_S are coordinates of centroid and shear centre respectively, and $\bar{u} = \bar{u}(x,y,z)$ is the cross-section warping intensity reduced to the wetted surface [4,5]. Symbols **i**, **j** and **k** denote unit vectors. From Eq. (13) the expressions for transmitting nodal displacements from the beam model to the 3D FEM substructure model can be extracted

$$\begin{aligned} \delta_X &= \frac{\mathrm{d}w_v}{\mathrm{d}x}\left(Z - z_N\right) + \frac{\mathrm{d}w_h}{\mathrm{d}x}Y + \bar{u}\frac{\mathrm{d}\psi}{\mathrm{d}x}, \\ \delta_Y &= -w_h - \psi\left(Z - z_S\right), \\ \delta_Z &= -w_v + \psi Y. \end{aligned} \tag{14}$$

These displacements are then imposed to the aft and fore 3D FEM substructure boundaries, and stress concentrations, as result of their differences, is calculated.

2.2 Hydrodynamic model

The full detail description of the used hydrodynamic model is already given in a number of references as for instance [4,5]. However, for the sake of the paper to be self-containing, its outline is also presented here. The coupling procedure does not depend on the used hydrodynamic model, and is therefore described here for the zero speed case, as the simplest one. Harmonic hydroelastic problem is considered in frequency domain and therefore we operate with amplitudes of forces and displacements. In order to perform the coupling of structural and hydrodynamic models, it is necessary to express the external pressure forces in a convenient manner [13]. First, the total hydrodynamic force F^h has to be split into two parts: the first part F^R depending on the structural deformations, and the second one F^{DI} representing the pure excitation. Furthermore, the modal superposition method can be used. Vector of the wetted surface deformations $\mathbf{H}\left(x,y,z\right)$ can be presented as a series of dry natural modes $\mathbf{h}_i(x, y, z)$. The potential theory assumptions are adopted for the hydrodynamic part of the problem. Within this theory, the total velocity potential φ, in the case of no forward speed, is defined with the Laplace differential equation and the given boundary values. Furthermore, the linear wave theory enables the following decomposition of the total potential

$$\varphi = \varphi_I + \varphi_D - i\omega\sum_{j=1}^{N}\xi_j\varphi_{Rj}, \qquad \varphi_I = -i\frac{gA}{\omega}\mathrm{e}^{\nu(z+ix)}, \tag{15}$$

where φ_I is incident wave potential, φ_D is diffraction potential, φ_{Rj} is radiation potential, ξ_j are modal amplitudes, g represents gravity constant, ν is wave number, and A and ω represent wave amplitude and frequency respectively. Once the potentials are determined, the modal hydrodynamic forces are calculated by pressure work integration over the wetted surface, S. The total linearized pressure can be found from Bernoulli's equation

$$p = i\omega\rho\varphi - \rho gz, \tag{16}$$

where ρ is fluid density.

First, the term associated with the velocity potential φ is considered and subdivided into excitation and radiation parts

$$F_i^{DI} = i\omega\rho\iint_S(\varphi_I + \varphi_D)\mathbf{h}_i\mathbf{n}\,\mathrm{d}S, \tag{17}$$

$$F_i^R = \rho\omega^2\sum_{j=1}^{N}\xi_j\iint_S\varphi_{Rj}\mathbf{h}_i\mathbf{n}\,\mathrm{d}S, \tag{18}$$

where **n** represents unit normal vector of the wetted surface S. Thus, F_i^{DI} represents the modal pressure excitation. Now one can decompose (18) into the modal inertia force and damping force associated with acceleration and velocity, respectively

$$F_i^a = \mathrm{Re}(F_i^R) = \omega^2\sum_{j=1}^{N}\xi_j A_{ij}, \qquad A_{ij} = \rho\,\mathrm{Re}\iint_S\varphi_{Rj}\,\mathbf{h}_i\mathbf{n}\mathbf{d}S, \tag{19}$$

$$F_i^v = \mathrm{Im}(F_i^R) = \omega\sum_{j=1}^{N}\xi_j B_{ij}, \qquad B_{ij} = \rho\omega\,\mathrm{Im}\iint_S\varphi_{Rj}\,\mathbf{h}_i\mathbf{n}\mathbf{d}S. \tag{20}$$

where A_{ij} and B_{ij} are elements of added mass and damping matrices respectively. Determination of added mass and damping for rigid body modes is a well-known procedure in ship hydrodynamics. Now the same procedure is extended to the calculation of these quantities for elastic modes. The hydrostatic part of the total pressure, $-\rho gz$ in (16), is considered within the hydrostatic model.

2.3 Hydrostatic model

Although hydroelasticity represents known issue for many years, there is still no unique solution for restoring stiffness which plays dominant role in hydrostatic model. There are several restoring stiffness formulations as, for example, the formulation of Price & Wu [14], Newman's formulation [15], formulations of Huang & Riggs [16], Malenica [17], Senjanović et al. [18,19]. In this investigation, a physically consistent formulation of restoring stiffness for application to ship structures, developed recently by Senjanović et al. [18], is used.

According to [18], the restoring stiffness consists of hydrostatic and gravity parts. Work of hydrostatic pressure, which represents the generalized force, can be derived in the following form

$$F^h = -\rho g\iint_S\left[H_z + Z\left(\nabla\mathbf{H}\right)\right]\mathbf{H}\mathbf{n}\mathrm{d}S, \tag{21}$$

where ∇ is Hamilton differential operator, **H** is displacement vector and H_z represents its vertical component, dS is differential of wetted surface, Z is its depth (distance from waterline) and **n** is unit normal vector. According to definition, the stiffness is relation between incremental force and displacement, so it is determined from the variational equation

$$\delta F^h = -\rho g\iint_S\left[H_z + Z\left(\nabla\mathbf{H}\right)\right]\delta\mathbf{H}\mathbf{n}\mathrm{d}S. \tag{22}$$

Furthermore, the modal superposition method is used, and the variation is transmitted to modes, i.e. modal forces and displacements

$$\delta F^h = \sum_{j=1}^{N}\delta F_j^h, \quad \mathbf{H} = \sum_{j=1}^{N}\xi_j\mathbf{h}_j, \quad \delta\,\mathbf{H} = \sum_{j=1}^{N}\mathbf{h}_j\delta\xi_j. \tag{23}$$

In that way, the first of Eqs. (23) is decomposed into the modal equations

$$\delta F_i^h = -\sum_{j=1}^{N}\left[\left(C_{ij}^p + C_{ij}^{nh}\right)\xi_j\right]\delta\xi_i, \tag{24}$$

where

$$C_{ij}^p = \rho g \iint_S \mathbf{h}_i h_z^j \mathbf{n}\mathrm{d}S, \tag{25}$$

$$C_{ij}^{nh} = \rho g \iint_S Z\mathbf{h}_i\left(\nabla\mathbf{h}_j\right)\mathbf{n}\mathrm{d}S, \tag{26}$$

are stiffness coefficients due to pressure, and normal vector and mode contributions, respectively.

Similar to the pressure part, the generalized gravity force reads

$$F^m = -g\iiint_V \rho_s\left(\mathbf{H}\nabla\right)H_z\mathrm{d}V, \tag{27}$$

where ρ_s and V are structure density and volume respectively. In order to obtain a consistent variational equation, it is necessary to strictly follow the definition of stiffness and to vary the displacement vector in (27) and not its derivatives

$$\delta F^m = -g\iiint_V \rho_s\left(\delta\mathbf{H}\nabla\right)H_z\mathrm{d}V. \tag{28}$$

Application of the modal superposition method leads to the modal variational equation

$$\delta F_i^m = -\sum_{j=1}^{N} C_{ij}^m \xi_j \delta\xi_i, \tag{29}$$

where

$$C_{ij}^m = g\iiint_V \rho_s\left(\mathbf{h}_i\nabla\right)h_z^j\mathrm{d}V, \tag{30}$$

are the gravity stiffness coefficients. Finally, the complete restoring stiffness coefficients are obtained by summing up its constitutive parts

$$C_{ij} = C_{ij}^p + C_{ij}^{nh} + C_{ij}^m. \tag{31}$$

2.4 Hydroelastic model

The governing modal matrix differential equation for coupled ship motions and vibrations yields:

$$\left[\mathbf{k} + \mathbf{C} - i\omega\left(\mathbf{d} + \mathbf{B}(\omega)\right) - \omega^2\left(\mathbf{m} + \mathbf{A}(\omega)\right)\right]\xi = \mathbf{F}, \tag{32}$$

where **k**, **d**, and **m** are modal structural stiffness, damping and mass matrices, respectively, **C** is restoring stiffness, **B**(ω) is hydrodynamic damping, **A**(ω) is modal added mass, ξ are modal amplitudes, **F** is modal wave excitation, and ω is encounter frequency which in case of no forward speed is equal to wave frequency.

3 Computer programs

Based on the developed theory computer programs have been developed. Both the theory and the programs have been checked by correlation analysis of the simulation results and the measured ones for a flexible segmented barge consisting of 12 pontoons, for which tests results are available [13,20]. Stiffness properties of ship hull are determined by program STIFF, based on the advanced theory of thin-walled girders, Figure 4 [21]. It calculates cross-section area, moments of inertia of cross-section, shear areas, torsional modulus, warping modulus, and shear inertia modulus, for both closed and opened cross-sections. The effective values of the above quantities can be also determined for the assumed sinusoidal modes. For the hydroelastic analysis DYANA program has been developed, based on the advanced beam theory and finite element technique, taking shear, bending, pure torsion, shear torsion and warping of cross-section into account [23]. The hydrodynamic part in DYANA has been taken from the program HYDROSTAR and adopted for hydroelastic analysis [23].

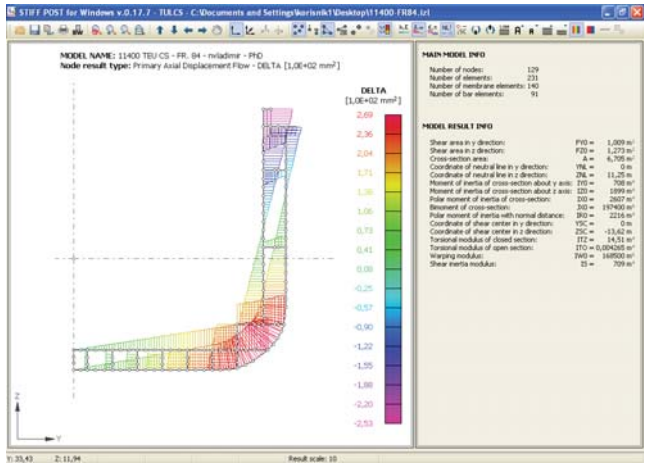

Figure 4 **Warping of ship cross-section – program STIFF**
Slika 4 **Vitoperenje poprečnog presjeka broda – program STIFF**

4 Numerical example

4.1 Ship particulars

A large container ship of 11400 TEU is considered, Figure 5. The main vessel particulars are the following:

Length overall	L_{oa} = 363.44 m
Length between perpendiculars	L_{pp} = 348.00 m
Breadth	B = 45.6 m
Depth	H = 29.74 m
Draught	T = 15.5 m
Displacement, full load	Δ_f = 171445 t
Displacement, ballast	Δ_b = 74977 t
Engine power	P = 72240 kW
Ship speed	v = 24.7 kn.

4.2 Beam model verification

The reliability of the beam model, which includes shear influence on both bending and torsion, and rotary inertia, is checked by correlating the lightship and full load dry natural frequencies, Tables 1 and 2, and mode shapes with those of 3D FEM analysis performed by NASTRAN [24], Figures 6, 7, 8 and 9. Very good agreement of the results can be noticed. However, somewhat less perfect agreement of dry natural frequencies for both vertical and coupled horizontal and torsional vibrations compared to the results for the light ship, despite the excellent similarity of the global inertial properties, can most probably be assigned to the way the (cargo) masses are modelled in the 3D model. Moreover, it should be mentioned that coupled horizontal and torsional vibrations of ULCS are much complex to simulate numerically comparing to vertical vibrations. The results of calculation of transverse bulkheads contribution to the hull stiffness is given in the Appendix.

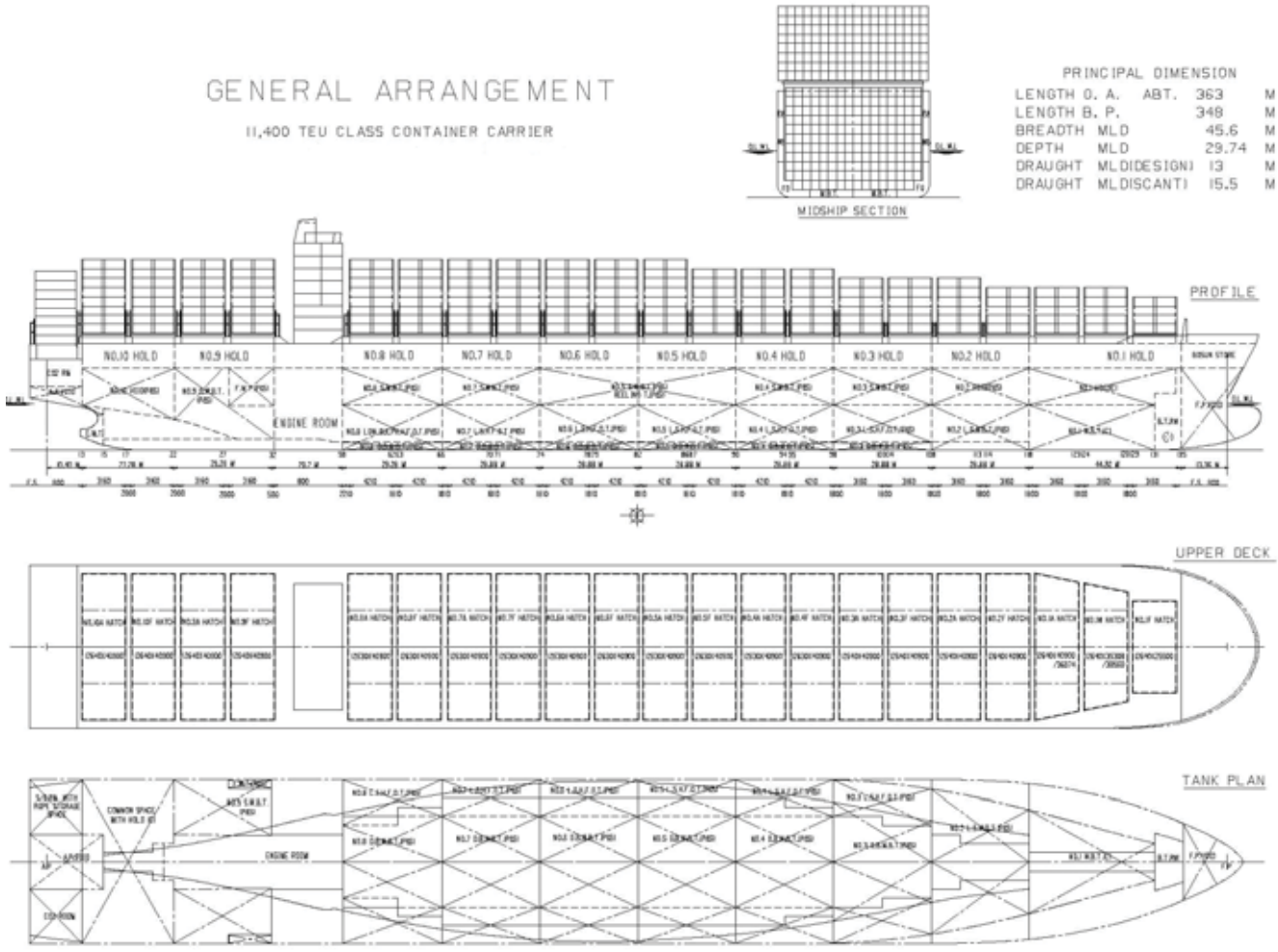

Figure 5 **The 11400 TEU container ship**
Slika 5 **Kontejnerski brod nosivosti 11400 kontejnera**

Table 1 **Dry natural frequencies of the light container ship (rad/s)**
Tablica 1 **Suhe prirodne frekvencije lakog kontejnerskog broda (rad/s)**

	1D		3D		Discrepancy, %	
No.	Vertical	Coupled	Vertical	Coupled	Vertical	Coupled
1	7.219	4.021	0.728	4.015	-0.86	0.16
2	14.564	6.616	14.627	6.761	-0.43	-2.14
3	23.210	10.920	22.959	10.996	1.09	-0,69

Table 2 **Dry natural frequencies of the fully loaded container ship (rad/s)**
Tablica 2 **Suhe prirodne frekvencije potpuno nakrcanog kontejnerskog broda (rad/s)**

	1D		3D		Discrepancy, %	
No.	Vertical	Coupled	Vertical	Coupled	Vertical	Coupled
1	3.682	1.923	3.682	2.061	0.00	-6.71
2	7.665	3.167	7.282	2.953	5.26	7.23
3	12.051	4.907	12.328	4.976	-2.26	-1.39

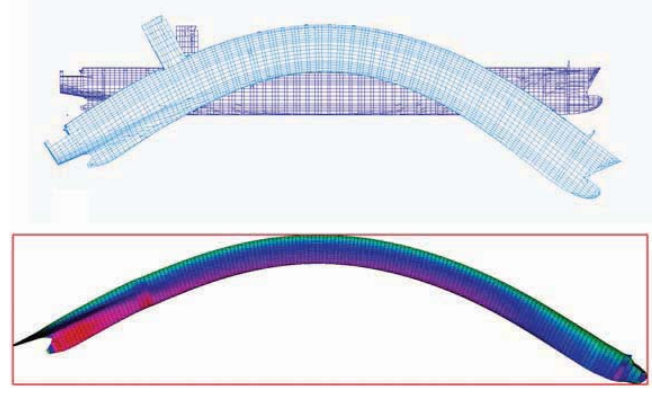

Figure 6 **The first lightship vertical vibration natural mode**
Slika 6 **Prvi prirodni oblik vertikalnih vibracija lakog broda**

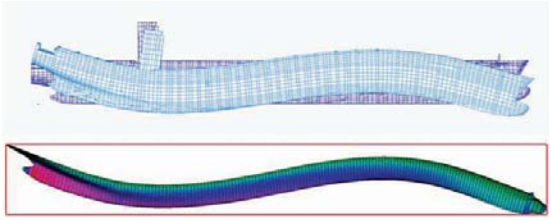

Figure 7 **The second lightship vertical vibration natural mode**
Slika 7 **Drugi prirodni oblik vertikalnih vibracija lakog broda**

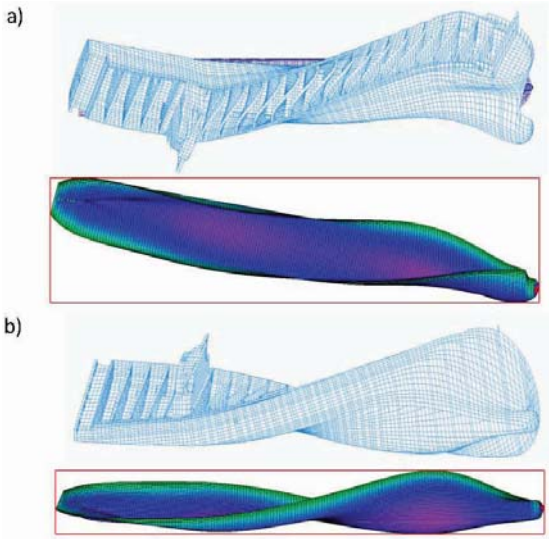

Figure 8 **The first lightship coupled horizontal and torsional vibration natural mode; a) bird's eye view, b) lateral view**
Slika 8 **Prvi prirodni oblik spregnutih horizontalnih i torzijskih vibracija lakog broda; a) pogled odozgo, b) bočni pogled**

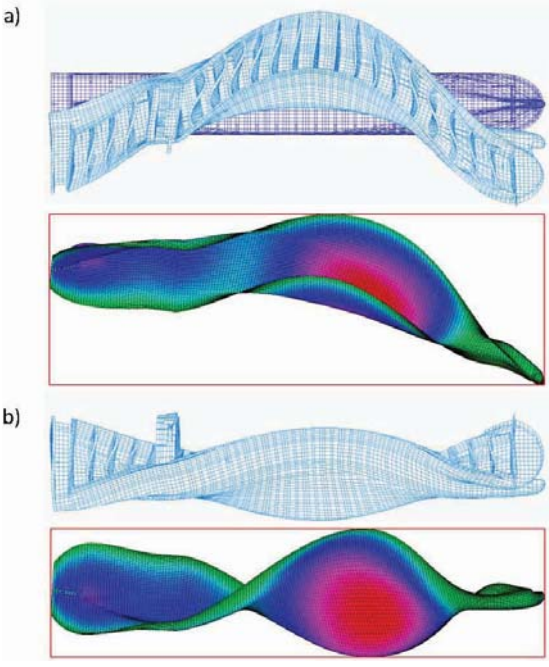

Figure 9 **The second lightship coupled horizontal and torsional vibration natural mode; a) bird's eye view, b) lateral view**
Slika 9 **Drugi prirodni oblik spregnutih horizontalnih i torzijskih vibracija lakog broda; a) pogled odozgo, b) bočni pogled**

4.3 Global hydroelastic response

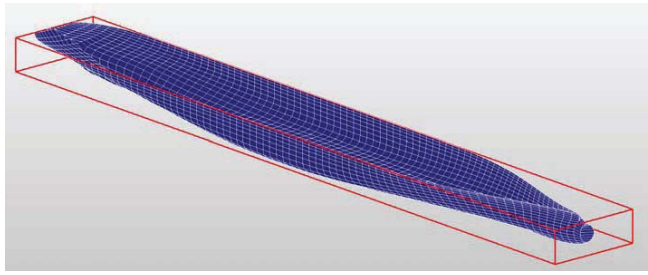

Figure 10 **Wetted surface of hydrodynamic model**
Slika 10 **Oplakana površina hidrodinamičkog modela**

Table 3. **Wet natural frequencies of fully loaded container ship (rad/s)**
Tablica 3 **Mokre prirodne frekvencije poptuno nakrcanog kontejnerskog broda (rad/s)**

No.	Vertical	Coupled
1	2.792	1.812
2	5.724	2.781
3	9.036	4.453

The wetted surface of the hydrodynamic model of the considered ship, which is necessary for hydroelastic calculations, is presented in Figure 10. The wet natural frequencies of the fully loaded container ship with the corresponding mass of 171445 t are presented in Table 3. Numerical calculation of ship response to waves is performed for several loading conditions, unit harmonic wave amplitude, and set of heading angles, ship speeds, and wave lengths. Here, only some selected results are presented. The transfer functions of vertical bending moment, horizontal bending moment, and torsional moment at the midship section, obtained using 1D FEM + 3D BEM hydroelastic model for the case of fully loaded ship (mass equal to 171445 t) and maximum ship speed (U=24.7 kn) are shown in Figures 11, 12 and 13, respectively.

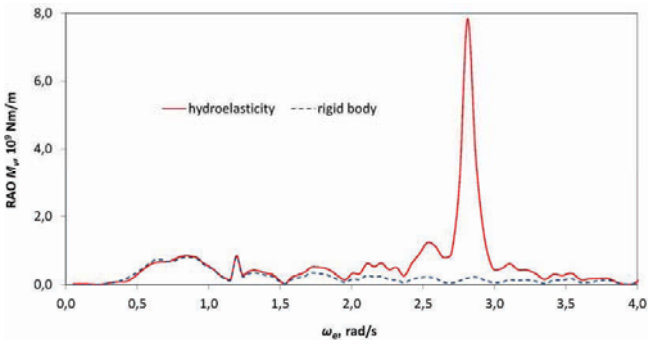

Figure 11 **Transfer function of vertical bending moment, x=120°, U=24.7 kn, x=175 m from AP**
Slika 11 **Prijenosna funkcija vertikalnog momenta savijanja, x=120°, U=24,7 čv, x=175 m od A.P.**

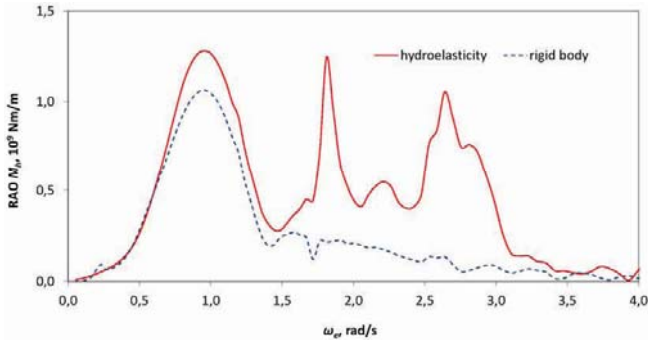

Figure 12 **Transfer function of horizontal bending moment, *x*=120°, *U*=24.7 kn, *x*=175 m from AP**
Slika 12 **Prijenosna funkcija horizontalnog momenta savijanja, *x*=120°, *U*=24,7 čv, *x*=175 m od A.P.**

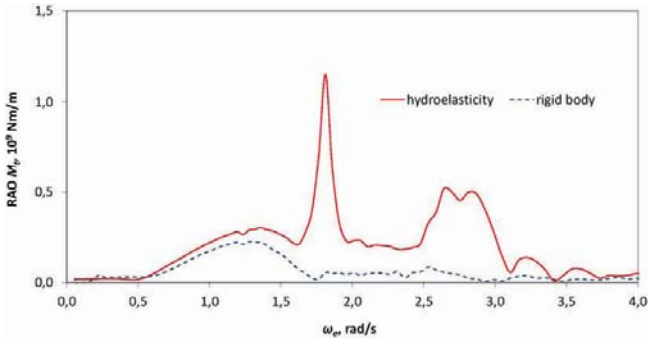

Figure 13 **Transfer function of torsional moment, *x*=120°, *U*=24.7 kn, *x*=175 m from AP**
Slika 13 **Prijenosna funkcija momenta uvijanja, *x* =120°, *U*=24,7 čv, *x*=175 m od A.P.**

The angle of 180° corresponds to the head sea. They are compared to the rigid body ones determined by program HYDROSTAR [23]. Very good agreement is obtained in the lower frequency domain, where the ship behaves as a rigid body, while large discrepancies occur at the resonances of the wet natural frequency of the elastic modes and encounter wave frequency, as expected. Further on, hydroelastic response obtained by 1D FEM + 3D BEM hydroelastic model is compared to the one obtained by fully coupled 3D FEM + 3D BEM hydroelastic model, Figures 14, 15 and 16, where quite good agreement is obvious. In this particular case, the loading condition No. 7 from the trim and stability book, which corresponds to ship mass of 136458 t, and a lower ship speed (U=15.75 kn) was selected. In case of vertical vibrations analysed with 1D model, Figure 14, larger discrepancies can be noticed in the vicinity of encounter frequency of 3.0 rad/s, but they are influenced by numerical instability. Namely, to overcome these shortcomings in the high frequency one should increase the number of panels in the hydrodynamic model to keep the accuracy level, which is rather time consuming. It should be mentioned that within the numerical examples the structural damping has been neglected, since its influence on the response is of the second order. However, it can be taken into account as 2 or 3 percent of critical damping.

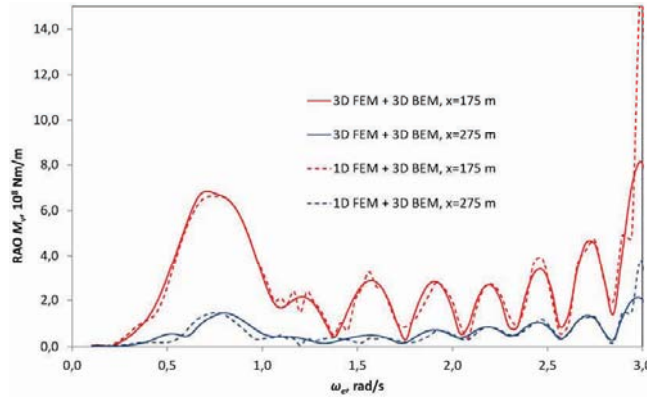

Figure 14 **Transfer function of vertical bending moment, *x*=120°, *U*=15.75 kn**
Slika 14 **Prijenosna funkcija vertikalnog momenta savijanja, *x*=120°, *U*=15,75 čv**

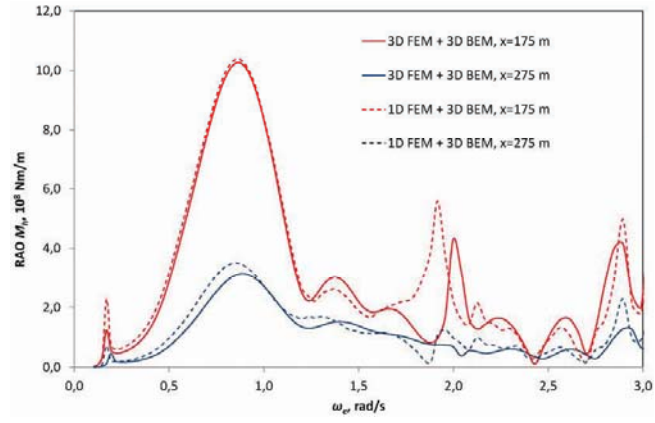

Figure 15 **Transfer function of horizontal bending moment, *x*=120°, *U*=15.75 kn**
Slika 15 **Prijenosna funkcija horizontalnog momenta savijanja, *x* =120°, *U*=15,75 čv**

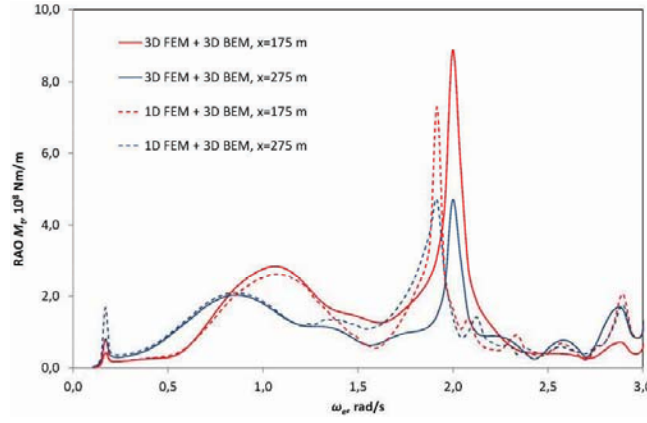

Figure 16 **Transfer function of torsional moment, *x*=120°, *U*=15.75 kn**
Slika 16 **Prijenosna funkcija momenta uvijanja, *x* =120°, *U*=15,75 čv**

4.4 Local response

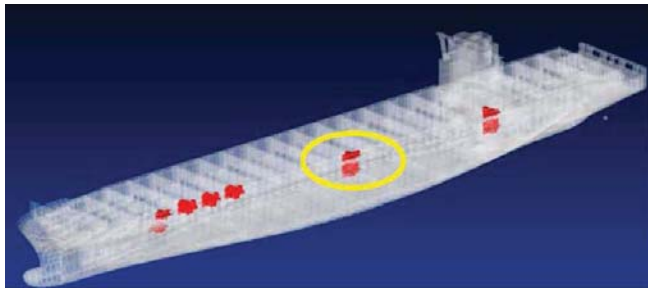

Figure 17 **Longitudinal position of the selected structural detail**
Slika 17 **Uzdužni položaj odabranog strukturnog detalja**

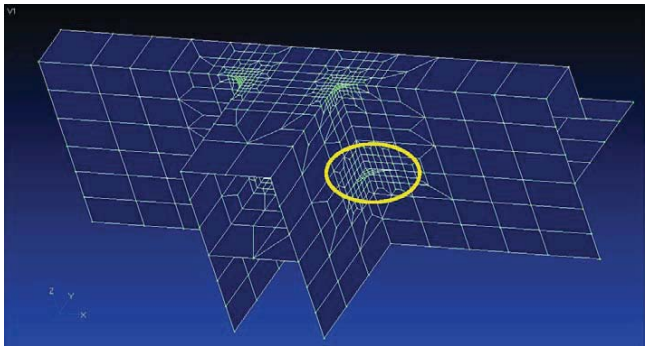

Figure 18 **Fine mesh of the selected structural detail**
Slika 18 **Odabrani detalj konstrukcije s ufinjenom mrežom**

The selected structural detail for the stress concentration assessment is a knee in the hatch corner at the upper deck level in the middle part of the ship, Figures 17 and 18, with full detail description in [6]. For the stress concentration analysis a 3D FEM substructure model with refined mesh in the vicinity of the selected structural detail has been built in program NASTRAN [24], and its deformed presentation is given in Figures 19 and 20. The local load, i.e.

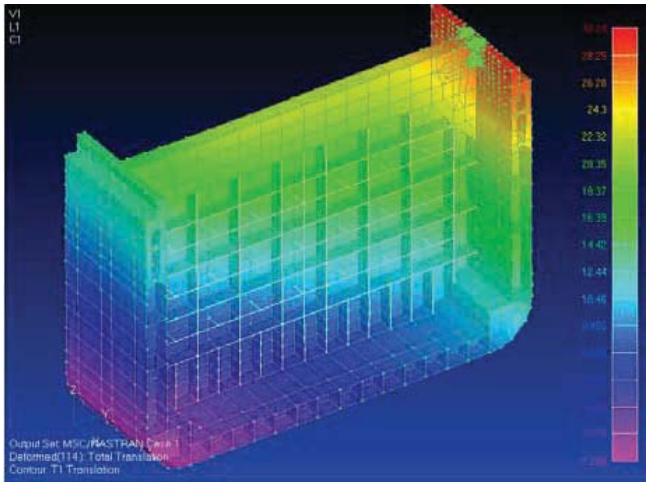

Figure 19 **Deformed substructure model, ω=0.90 rad/s, real component of the response**
Slika 19 **Deformirani model podstrukture, ω=0,90 rad/s, realna komponenta odziva**

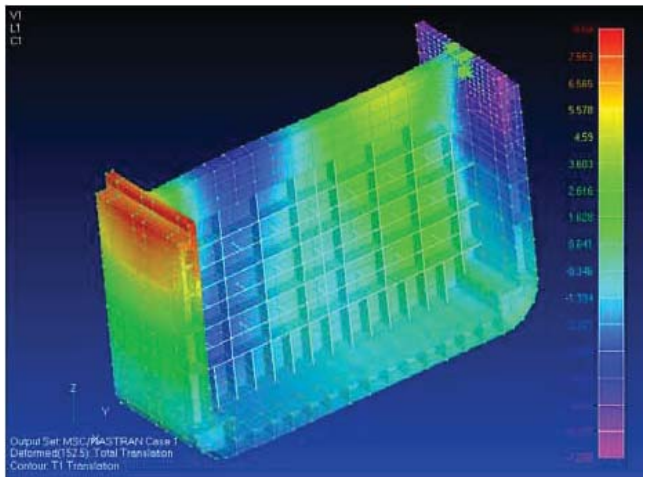

Figure 20 **Deformed substructure model, ω=0.90 rad/s, imaginary component of the response**
Slika 20 **Deformirani model podstrukture, ω=0,90 rad/s, imaginarna komponenta odziva**

the weight of containers on the hatch coamings and water pressure, are not taken into account due to the reason of simplicity. This simplification should not significantly influence the results due to the fact that the values of cross-section forces (as well as displacements) are several times higher than the values of container weights and pressure loads, if the substructure is relatively short as in the considered case. It should be mentioned that the real and imaginary components of the response should be calculated separately, and at the end, at the level of stresses should be summed up as complex numbers. Figures 21 and 22 show the stress distributions in the considered structural detail. The analyzed stress is normal stress along the knee boundary. In order to register it, bar elements of negligible stiffness are fitted on the knee boundary. Transfer functions of stress concentrations obtained by 1D FEM +3D BEM and 3D FEM + 3D BEM hydroelastic models are presented in Figure 23. In the low frequency domain rather high discrepancies can be noticed, while in the high frequency domain, where the springing influence on fatigue damage accumulation is pronounced, quite good agreement is achieved.

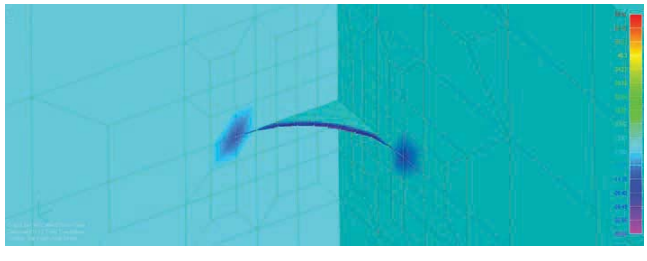

Figure 21 **Stress distribution in the structural detail, ω=0.90 rad/s, real component**
Slika 21 **Distribucija naprezanja detalja konstrukcije, ω=0,90 rad/s, realna komponenta**

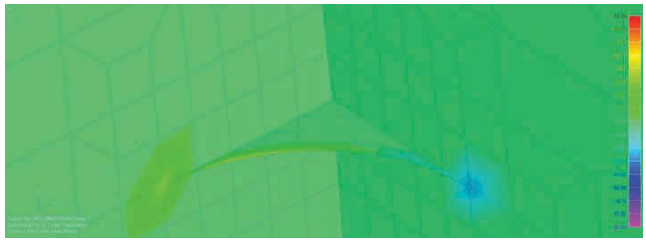

Figure 22 **Stress distribution in the structural detail, *x*=0.90 rad/s, imaginary component**
Slika 22 **Distribucija naprezanja detalja konstrukcije, *x*=0,90 rad/s, imaginarna komponenta**

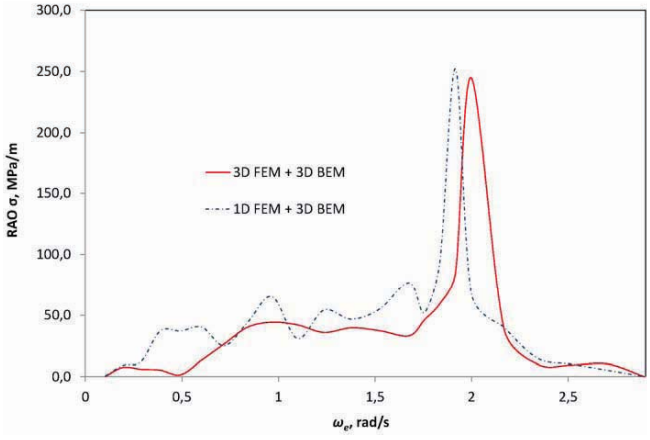

Figure 23 **Transfer functions of stress concentration**
Slika 23 **Prijenosne funkcije koncentracije naprezanja**

5 Conclusion

ULCS are rather flexible and quite fast, so they have to be submitted to hydroelastic analysis. A previously developed hydroelastic model, based on a sophisticated beam model and a 3D BEM hydrodynamic model, which is proven to be reliable for the global hydroelastic response calculations, can be extended for the assessment of stress concentrations in combination with a 3D FEM substructure model. It should be emphasized that the stress transfer function determining represents the first step in the fatigue damage assessment which is quite complex problem itself. The idea applied in this investigation is to calculate the deflection amplitudes of the selected cross-sections for each encounter frequency assuming a beam structural model, and then spread them to the cross-section contours. After that, they should be imposed as boundary conditions at the 3D FEM substructure fore and aft side. Finally, the stresses in the selected structural detail, as a result of different deflections on the 3D FEM substructure contours, can be obtained. Although the proposed procedure gives acceptable agreement of the stress levels, especially in the high frequency range where springing influence is pronounced, some improvements are still needed in the low frequency domain to increase the accuracy of the fatigue damage calculation which should follow.

In order to complete hydroelastic analysis of container ships and confirm its importance for ship safety, it is necessary to proceed further to ship motion calculation in irregular waves for different sea states, based on the known transfer functions. At the end of a complete investigation, which also has to include model tests and full-scale measurements, it will be possible to decide on the extent and improvement of Classification Rules for the design and construction of ultra large container ships.

Appendix – Contribution of transverse bulkheads

Table A.1 **Stiffness parameters of watertight bulkhead**
Tablica A.1 **Parametri krutosti nepropusne pregrade**

Girder	Moment of inertia	Torsional modulus	Girder spacing	Moment of inertia per unit breadth	Torsional modulus per unit breadth
	I (m^4)	I_t (m^4)	c (m)	i (m^3)	i_t (m^3)
Horizontal	0.0216	0.00905	5.184	0.004164	0.002843
Vertical	0.03094	0.023328	5.04	0.006139	

Table A.2 **Stiffness parameters of support bulkhead**
Tablica A.2 **Parametri krutosti propusne pregrade**

Girder	Moment of inertia	Torsional modulus	Girder spacing	Moment of inertia per unit breadth	Torsional modulus per unit breadth
	I (m^4)	I_t (m^4)	c (m)	i (m^3)	i_t (m^3)
Horizontal	0.00972	0.00486	5.184	0.001875	0.002293
Vertical	0.02017	0.02827	5.04	0.004002	

Table A.3 **Stool stiffness parameters**
Tablica A.3 **Parametri krutosti kutije pregrade**

Shear area	Moment of inertia	Torsional modulus
A_s (m^2)	I_s (m^4)	I_{ts} (m^4)
0.045	0.12236	0.433

The ship is designed with alternate watertight and support bulkheads, and their contribution to the hull stiffness is assessed according to theoretical model presented in Chapter 2. The stiffness parameters of the bulkhead girders are listed in Tables A.1 and A2, while the stool parameters are given in Table A.3. The bulkhead dimensions are the following: H = 29.44 m, b = 20.45 m, l_0 = 14.44 m, α = 1.80 m.

Table A.4 **Bulkhead strain energy, (U / ($E\psi^{i2}$)**
Tablica A.4 **Energija deformacije pregrade, (U / ($E\psi^{i2}$)**

Watertight bulkhead		Support bulkhead		Energy coefficient
Grillage	Stool	Grillage	Stool	C, Eq. (C5)
(1)	(2)	(3)	(4)	(5) = [(1)+(2)+(3)+ (4)]/2
22.248	60.437	11.059	60.437	77.191

The bulkhead strain energy, determined according to Eqs. (8) and (9), is summarized in Table A.4, where also the energy coefficient is calculated as the average value of the watertight and support bulkhead strain energies. Most of the hull induced energy is absorbed by the stool. Thus, the equivalent torsional modulus

for midship section yields $I_t^* = 1.9 I_t$. This value is applied for all ship cross-sections as the first approximation.

Acknowledgment

This work was supported by the National Research Foundation of Korea (NRF) grant funded by the Korea Government (MEST) through GCRC-SOP (Grant No. 2011-0030669). The authors express their gratitude to Mr. Fabien Bigot, *Bureau Veritas*, Paris, for performing the 3D FEM + 3D BEM hydroelastic analysis of the 11400 TEU container ship.

References

[1] MALENICA, Š., SENJANOVIĆ, I., DERBANNE, Q., VLADIMIR, N.: "On the EU FP7 Project: Tools for Ultra Large Container Ships – TULCS", Brodogradnja, Vol. 62, No. 2, 2011, p. 177-187.

[2] CHEN, X.J, WU, Y.S., CUI, W.C., JUNCHER JENSEN, J.: Review of hydroelasticity theories for global response of marine structures, Ocean Engineering, Vol. 33, 2006, p. 439-457.

[3] WU, Y.S., CUI, W.C.: Advances in three-dimensional hydroelasticity of ships, Proc. IMechE Part M: Journal of Engineering for the Maritime Environment, Vol. 223, No. 3, 2009, p. 331-348.

[4] SENJANOVIĆ, I., MALENICA, Š., TOMAŠEVIĆ, S.: "Investigation of ship hydroelasticity", Ocean Engineering, Vol. 35, 2008, p. 523-535.

[5] SENJANOVIĆ, I., MALENICA, Š., TOMAŠEVIĆ, S.: "Hydroelasticity of large container ships", Marine Structures, Vol. 22, No. 2, 2009, p. 287-314.

[6] BOUTILLIER, V., MAHERAULT, S., HUTHER, M., HENRY, J., PARMENTIER, G.: "Fatigue damage calculation of ULCS due to quasi-static wave response and springing response", Proceedings of the PRADS Conference, Rio de Janeiro, Brazil, 2010, p. 1190-1199.

[7] SENJANOVIĆ, I., TOMAŠEVIĆ, S., VLADIMIR, N.: "An advanced theory of thin-walled girders with application to ship vibrations", Marine Structures, Vol. 22, No. 3, 2009, p. 387-437.

[8] PAVAZZA, R.: "Torsion of thin-walled beams of open cross-sections with influence of shear", International Journal of Mechanical Sciences, Vol. 47, 2005, p. 1099-1122.

[9] PAVAZZA, R.: "Introduction to thin-walled beam analysis", Kigen, Zagreb, 2007. (in Croatian).

[10] SENJANOVIĆ, I., RUDAN, S., VLADIMIR, N.: "Influence of shear on the torsion of thin-walled girders", Transactions of FAMENA, Vol. 33, No. 2, 2009, p. 35-50.

[11] SENJANOVIĆ, I., TOMAŠEVIĆ, S., RUDAN, S., SENJANOVIĆ, T.: "Role of transverse bulkheads in hull stiffness of large container ships", Engineering Structures, Vol. 30, No. 9, 2008, p. 2492-2509.

[12] SENJANOVIĆ, I., VLADIMIR, N., TOMIĆ, M.: "Effective stiffness of the engine room structure in large container ships", Brodogradnja, Vol. 62, No. 1, 2011, p. 15-27.

[13] MALENICA, Š., MOLIN, B., REMY, F., SENJANOVIĆ, I.: "Hydroelastic response of a barge to impulsive and non-impulsive wave load", Proceedings of the International Conference on Hydroelasticity in Marine Technology, Oxford, UK, 2003, p. 107-115.

[14] PRICE, W.G., WU, Y.S.: "Hydroelasticity of Marine Structures", In Theoretical and Applied Mechanics, Niordson, F.I. and Olhoff, N. (eds), Elsevier Science Publishers BV, 1985, p.311-337.

[15] NEWMAN, J.N.: "Wave effects on deformable bodies", Applied Ocean Research, Vol. 16, 1994, p. 47-59.

[16] HUANG, L.L., RIGGS, H.R.: "The hydrostatic stiffness of flexible floating structure for linear hydroelasticity", Marine Structures, Vol. 13, 2000, p. 91-106.

[17] MALENICA, Š.: "Some aspects of hydrostatic calculations in linear seakeeping", Proceedings of the 14th NAV Conference, Palermo, Italy, 2003.

[18] SENJANOVIĆ, I., VLADIMIR, N., TOMIĆ, M.: "Formulation of consistent restoring stiffness in ship hydroelastic analysis", Journal of Engineering Mathematics, Vol. 72, No. 1, 2012, p. 141-157.

[19] SENJANOVIĆ, I., HADŽIĆ, N., VLADIMIR, N.: "Restoring stiffness in the hydroelastic analysis of marine structures", Brodogradnja, Vol. 62, No. 3, 2011, p. 265-279.

[20] REMY, F., MOLIN, B., LEDOUX, A.: "Experimental and numerical study of the wave response of a flexible barge", Proceedings of the International Conference on Hydroelasticity in Marine Technology, Wuxi, China, 2006, p. 255-264.

[21] …"STIFF", User's Manual. FAMENA, Zagreb, 2011.

[22] ..."DYANA", User's Manual. FAMENA, Zagreb, 2011.

[23] ..."HYDROSTAR", User's Manual. Bureau Veritas, Paris, 2006.

[24] ..."MSC.NASTRAN 2005", Installation and Operations Guide, MSC.Software, 2005.